Synthesis, Structure, and Applications of Transition-Metal Polyhydride Anions

Daniel Alvarez, Jr., Eric G. Lundquist, Joseph W. Ziller, William J. Evans,*,† and Kenneth G. Caulton*,‡

Contribution from the Departments of Chemistry, Indiana University, Bloomington, Indiana 47405, and University of California, Irvine, California 92717. Received March 6, 1989

Abstract: KH is used to deprotonate ReH_7L_2 (L = PMe_2Ph, $PMePh_2$, and PPh_3) and ReH_5P_3 and WH_6P_3 (P = PMe_2Ph) in THF, and the resulting anions are characterized by variable-temperature multinuclear NMR. The solid-state structure of $K(THF)_2ReH_6(PPh_3)_2$ was determined by X-ray diffraction and revealed a centrosymmetric dimer connected by bridging hydrogen atoms as follows: $\{[(Ph_3P)_2ReH_3](\mu\text{-H})[K(THF)_2]\}_2(\mu_3\text{-H})_4$. Crystallographic data (213 K): $a = 10.987$ (2), $b = 27.134$ (4), $c = 14.030$ (2) Å; $\beta = 96.609$ (13)°; $V = 4154.6$ (11) Å^3, and $Z = 2$ in space group $P2_1/n$. The reaction of KD with $ReH_7(PPh_3)_2$ gave HD and $ReH_6(PPh_3)_2^-$, thus supporting the idea that the synthetic reaction is in fact proton transfer and ruling out a mechanism consisting of addition of KD to unsaturated $ReH_5(PPh_3)_2$. $LiRuH_3(PPh_3)_3$ reacts with $^1/_2$-$[(COD)RhCl]_2$ to give $(COD)Rh(\mu\text{-H})_3Ru(PPh_3)_3$ as the kinetic product; this then rearranges ($t_{1/2} = 40$ min) in solution to give the thermodynamic isomer $(COD)RhH(\mu\text{-H})Ru(H)(PPh_3)_3$.

Heterobimetallic complexes have recently attracted considerable attention in light of the promise of enhanced reactivity due to cooperativity between adjacent, but electronically different, metal centers.[1-3] A large number of these bimetallic compounds have been synthesized by the reactions of organometallic halides with anionic metal carbonyls or phosphidometalates. However, only a few of these complexes have exhibited any catalysis or enhanced reactivity as a result of this mixed metal arrangement. This lack of reactivity is due in part to the absence of hydride ligands, which could reduce a coordinated substrate. We describe here some general features of the synthesis of transition-metal polyhydride anions[4-8] useful in the synthesis of hydride-rich heterobimetallic complexes. In addition, we describe a typical reaction of one of these anions with an organometallic halide to form a Rh–Ru polyhydride.

Experimental Section

All manipulations were carried out using standard Schlenk and glovebox procedures under prepurified nitrogen or vacuum. Bulk solvents (THF, benzene, toluene, pentane) were dried and deoxygenated by sodium or potassium benzophenone and vacuum transferred prior to use; deuterated THF and toluene were dried over sodium metal. KH is obtained as a dispersion in mineral oil (Aldrich). The oil is removed by washing the dispersion three times with pentane in a dry nitrogen atmosphere.[9] ^{1}H and ^{31}P NMR spectra were recorded on a Nicolet NT-360 spectrometer at 360 and 146 MHz, respectively, as well as on General Electric QE-300 and GN-500 MHz instruments. The polyhydride complexes, $WH_6(PMe_2Ph)_3$,[10] $ReH_7(PPh_2Me)_2$,[11] ReH_5-$(PMe_2Ph)_3$,[12] $OsH_4(PMe_2Ph)_3$,[13] and $ReH_7(PPh_3)_2$[14] were prepared by literature methods, as were $K[ReH_6(PPh_2Me)_2]^2$ and $K[OsH_3$-$(PMe_2Ph)_3]$.[2,7] In order to avoid protonation of these very basic anions, glassware was treated with Surfasil silylating reagent (Pierce Chemical Co.).

Synthesis of $OsH_4(PMe_2Ph)_3$. OsH_4P_3 (P = PMe_2Ph) can be synthesized in good yields from the reduction of *mer*-$OsCl_3(PMe_2Ph)_3$ with NaBH$_4$ in ethanol as reported[13] in the literature with one modification. Treating the $OsCl_3(PMe_2Ph)_3$ with NaBH$_4$ in ethanol at reflux as described in the literature was found to be unnecessary and actually diminished the yield. Stirring the $OsCl_3(PMe_2Ph)_3$/NaBH$_4$ mixture in ethanol at 25 °C until the red had disappeared (ca. 5 h) was found to produce high yields of $OsH_4(PMe_2Ph)_3$. $OsH_4(PMe_2Ph)_3$ does decompose in air over prolonged periods of time (weeks) and thus should be stored under N$_2$.

Synthesis of $K[ReH_4(PMe_2Ph)_3)]$. A 5-mm NMR tube containing 0.060 g (0.100 mmol) of $ReH_5(PMe_2Ph)_3$ and excess KH in THF-d_8 was heated in reflux (65 °C) for 24 h. The solution turned yellow over the course of heating. ^{1}H NMR (360 MHz, 20 °C, THF-d_8): −8.90 (q, J_{H-P} = 19 Hz, 4 H), 1.60 (d, J_{Me-P} = 3 Hz, 18 H), 7.0 (m, P–Ph), 7.6 (m, P–Ph). ^{31}P{^{1}H} NMR (146 MHz, 20 °C, THF-d_8): −18.0 (s).

Synthesis of $(THF)_xK[WH_5(PMe_2Ph)_3]$. A 5-mm NMR tube containing 0.060 g (0.100 mmol) of $WH_6(PMe_2Ph)_3$ and excess KH in THF-d_8 was allowed to react for 20 h at room temperature. The pale yellow solution turns an orange-red and then a dark, blood red color. ^{1}H NMR (360 MHz, 19 °C, THF-d_8): −4.80 (br m, 5 H), 1.65 (br d, J_{Me-P} = 9 Hz, 18 H), 7.15 (m, P–Ph), 7.70 (m, P–Ph). ^{31}P{^{1}H} NMR (146 MHz, 20 °C, THF-d_8): −0.50 (s, J_{P-W} = 167 Hz). Low-temperature ^{1}H NMR (360 MHz, −85 °C, THF-d_8): −5.00 (m), −4.10 (br m), 1.65 (d, J_{Me-P} = 9 Hz), 7.15 (m, P–Ph), 7.70 (m, P–Ph). ^{31}P{^{1}H} NMR (146 MHz, −90 °C, THF-d_8): +1.40 (d, J_{P-P} = 18 Hz, 2 P), −8.15 (t, J_{P-P} = 18 Hz, 1 P).

$\{K(THF)_2ReH_6(PPh_3)_2\}_2$. To a THF solution of $ReH_7(PPh_3)_2$ was added a 3-fold excess of KH. Reaction occurred immediately, and the resulting yellow-green solution was allowed to stir at room temperature for 30 min. The excess KH may be removed by filtration or centrifugation, and THF solvent was removed in vacuo to yield a green oily solid. This solid was washed with 4:1 hexane/THF to give a yellow powder. Alternatively, a 4-fold excess of hexane may be layered over a THF solution containing $\{K(THF)_2ReH_6(PPh_3)_2\}_2$ (1), and the resulting solution held at −35 °C for 90 h to yield light green X-ray quality crystals of (1). ^{1}H NMR (C_6D_6, 25 °C) of the green oily solid shows that conversion to $\{K(THF)_2ReH_6(PPh_3)_2\}_2$ is nearly quantitative. ^{1}H NMR (C_6D_6): 7.78 (t, J = 7 Hz, P–Ph), 6.97 (t, J = 7 Hz, P–Ph), 6.92 (t, J = 7 Hz), 3.56 (m, free THF), 1.41 (m, free THF), −7.22 (t, J = 14 Hz, Re–H). ^{31}P{^{1}H} NMR: 36.36 (s).

The deprotonation proceeds similarly for 200 mg of $ReH_7(PMe_2Ph)_2$ in 20 mL of THF. After the reaction is complete, excess KH is removed

(1) Roberts, D. A.; Geoffroy, G. L. *Comprehensive Organometallic Chemistry*, Wilkinson, G., Stone, F. G. A., Abel, W. W., Eds.; Pergamon Press: Oxford, 1982; Chapter 40.

(2) Bruno, J. W.; Huffman, J. C.; Green, M. A.; Caulton, K. G. *J. Am. Chem. Soc.* **1984,** *106,* 8310, and references therein. See also: Ben Laarab, H.; Chaudret, B.; Delavaux, B.; Dahan, F.; Poilblanc, R.; Taylor, N. J. *New J. Chem.* **1988,** *12,* 435. Meuting, A. M.; Bos, W.; Alexander, B. D.; Bogle, P. D.; Casalnuovo, J. A.; Balaban, S.; Ito, L. N.; Johnson, S. M.; Pignolet, L. H. *New J. Chem.* **1988,** *12,* 505.

(3) Lundquist, E. G.; Huffman, J. C.; Caulton, K. G. *J. Am. Chem. Soc.* **1986,** *108,* 8309.

(4) Chan, A. S. C.; Shieh, H.-S. *J. Chem. Soc., Chem. Commun.* **1985,** 1379.

(5) Bandy, J. A.; Berry, A.; Green, M. L. H.; Prout, K. *J. Chem. Soc., Chem. Commun.* **1985,** 1462. Barron, A. R.; Hursthouse, M. B.; Motevalli, M.; Wilkinson, G. *J. Chem. Soc., Chem. Commun.* **1986,** 81.

(6) $KReH_6(PPh_3)_2$ has been reported and coupled with Cp_3UCl. See: Baudry, D.; Ephritikhine, M. *J. Organomet. Chem.* **1986,** *311,* 189.

(7) Huffman, J. C.; Green, M. A.; Kaiser, S. L.; Caulton, K. G. *J. Am. Chem. Soc.* **1985,** *107,* 5111.

(8) Lin, D. E.; Halpern, J. *J. Am. Chem. Soc.* **1987,** *109,* 2974.

(9) Inkrott, K.; Goetze, R.; Shore, S. G. *J. Organomet. Chem.* **1978,** *154,* 337.

(10) Crabtree, R. H.; Hlatky, G. G. *Inorg. Chem.* **1984,** *23,* 2388.

(11) Skupinski, W. A.; Huffman, J. C.; Bruno, J. W.; Caulton, K. G. *J. Am. Chem. Soc.* **1984,** *106,* 8128.

(12) Douglas, P. G.; Shaw, B. L. *Inorg. Synth.* **1977,** *17,* 64.

(13) Douglas, P. G.; Shaw, B. L. *J. Chem. Soc. A* **1970,** 334.

(14) Cameron, C. J.; Moehring, G. A.; Walton, R. A. *Inorg. Synth.*, in press.

† University of California.
‡ Indiana University.

by filtration, and the filtrate is cooled to precipitate the pale yellow salt. IR (Nujol): 1825 (s, br). $^{31}P\{^1H\}$ NMR (THF): -13.8. ^1H NMR (THF = d_8, 360 MHz): 7.75, 7.1 (m); 1.68 (d, J = 6.5 Hz, PMe); -8.34 (t, J = 15.5, Re-H).

$KReH_6(PPh_3)_2$. $\{K(THF)_2ReH_6(PPh_3)_2\}_2$ was dissolved in an excess of toluene. This solvent was then removed in vacuo to yield $KReH_6$-$(PPh_3)_2$ (**2**) as a green powder. By the absence of THF, the ^1H NMR of **2** shows this conversion to be quantitative. Attempts to grow X-ray quality crystals of (**2**) from several hexane/toluene mixtures were unsuccessful. ^1H NMR (C_6D_6): 7.78 (t, J = 7 Hz, P-Ph), 6.97 (t, J = 7 Hz, P-Ph), 6.95 (t, J = 7 Hz, P-Ph), -7.21 (t, J = 14 Hz). $^{31}P\{^1H\}$ NMR: 36.36 (s).

Reaction of $ReH_7(PPh_3)_2$ with KD. (a) ^2H NMR Analysis. To a vial containing 50 mg (0.0697 mmol) of $ReH_7(PPh_3)_2$ and excess KD was added 10 mL of THF. This mixture was stirred for 20 s and then subjected to rotary evaporation for 30 s to remove the evolved gases. This procedure was repeated several times with stirring increments of 30 s, 1 min, and 5 × 2 min. After a total stirring time of 14 min, the reaction was stopped and THF solvent was removed in vacuo. The resulting green solid was extracted with four portions of benzene (0.90, 0.90, 0.92, 0.96 mL) totaling 3.68 mL. This was followed by extraction of the remaining white solid with 0.4 mL of THF. The THF solution was then added to the benzene solution. The latter step was performed in order to ensure complete extraction and solvation of $(KReH_6(PPh_3)_2 (THF)_2)_2$. The intensity of the Re-D peak (a broad singlet) in the ^2H NMR, integrated relative to natural-abundance deuterium in C_6H_6 solvent, revealed that only 2.60 atom % deuterium had been incorporated. $^{31}P-D$ coupling was not completely resolved.

(b) Mass Spectral Analysis. A flask containing $ReH_7(PPh_3)_2$ and excess KD was placed under vacuum (<10^{-5} atm). THF solvent was then vacuum transferred into the reaction flask, and the resulting solution was stirred for 20 min. The evolved gases were collected by Toepler pump methods. Mass spectrometry revealed the presence of HD as the major component of the gas mixture, along with minor amounts of H_2 and D_2.

Synthesis of $(COD)Rh(\mu-H)_3Ru(PPh_3)_3$. To a THF solution containing 0.100 g (0.11 mmol) of $Li[RuH_3(PPh_3)_3]^4$ was added solid $[(C-OD)RhCl]_2$ (0.050 g, 0.05 mmol). After the solution was stirred for 20 min, THF was removed under vacuum. This red-brown material was redissolved in 5 mL of benzene and filtered to remove LiCl. ^1H NMR (360 MHz, 20 °C, C_6D_6): -10.6 (second-order m, $AA'A''XX'X''M$, 3 H), 1.60 (m, CH_2 COD, 4 H), 2.30 (m, CH_2 COD, 4 H), 4.40 (s, vinyl COD, 4 H), 7.0-7.5 (m, P-Ph). $^{31}P\{^1H\}$ NMR (146 MHz, 20 °C, C_6D_6): 60.0 (s).

Synthesis of $(COD)RhH(\mu-H)RuH(PPh_3)_3$. Upon standing, a solution of $(COD)Rh(\mu-H)_3Rh(PPh_3)_3$ isomerizes ($t_{1/2}$ = 40 min) to give $(COD)RhH(\mu-H)RuH(PPh_3)_3$. ^1H NMR (360 MHz, 20 °C, C_6D_6) selective decoupling studies reveal the following: -14.20 (ddt, J_{H-Rh} = 31 Hz, J_{H-P} = 31 Hz, J_{H-P} = 16.5 Hz, 1H), -13.20 (td, J_{H-P} = 20 Hz, J_{H-P} = 16.5 Hz, 1 H), -9.80 (dm, J_{H-Rh} = 38 Hz, 1 H), 1.30 (m, CH_2 COD, 2 H), 1.55 (m, CH_2 COD, 2 H), 1.85 (m, CH_2 COD, 4 H), 3.75 (s, vinyl COD, 2 H), 4.70 (s, vinyl COD, 2 H), 7.0-8.0 (m, P-Ph). $^{31}P\{^1H\}$ NMR (146 MHz, 20 °C, C_6D_6): 56.1 (d, J_{P-P} = 24 Hz, 2 P), 65.0 (td, J_{P-P} = 24 Hz, J_{P-Rh} = 10 Hz, 1 P).

Collection of X-ray Diffraction Data. A yellow-green plate of approximate dimensions 0.10 × 0.20 × 0.40 mm was immersed in Paratone-N (a lubricating oil additive), mounted on a glass fiber and transferred to the Syntex $P2_1$ diffractometer, which is equipped with a modified LT-1 apparatus. Subsequent determination of accurate unit cell dimensions and orientation matrix and collection of low-temperature (213 K) intensity data were carried out using standard techniques similar to those of Churchill.[15] Final cell parameters are based on a least-squares analysis of 34 reflections in well-separated regions of reciprocal space, all having 24° < 2θ < 36°. Details are given in Table I.

All 5453 data were corrected for the effects of absorption and for Lorentz and polarization effects and placed on an approximately absolute scale by means of a Wilson plot. A careful survey of a preliminary data set revealed the systematic extinctions $0k0$ for k = 2n + 1 and $h0l$ for $h+l$ = 2n + 1; the diffraction symmetry was 2/m. The centrosymmetric monoclinic space group $P2_1/n$, a nonstandard setting of $P2_1/C_{2h}^5$ (No. 14), is thus uniquely defined.

Solution and Refinement of the Crystal Structure. All crystallographic calculations were carried out using either a locally modified version of the UCLA Crystallographic Computing Package[16] or the SHELXTL PLUS program set.[17] The analytical scattering factors for neutral atoms were
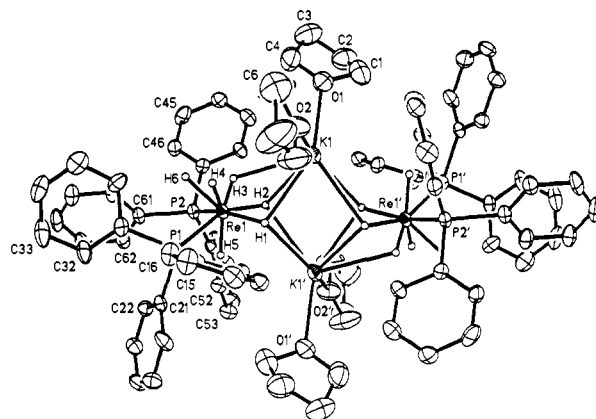
(15) Churchill, M. R.; Lashewycz, R. A.; Rotella, F. J. *Inorg. Chem.* **1977**, *16*, 265.

(16) UCLA Crystallographic Computing Package, University of California, Los Angeles, 1981. Strouse, C., personal communication.

(17) Nicolet Instrument Corp., Madison, WI, 1988.

Figure 1. ORTEP drawing of the complete centrosymmetric dimer {K-$(THF)_2ReH_6(PPh_3)_2\}_2$ in the solid state. Carbon-bound hydrogens have been omitted for clarity.

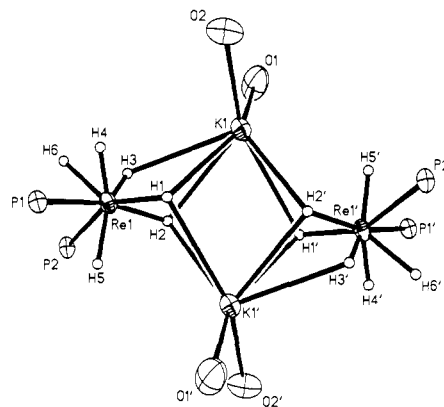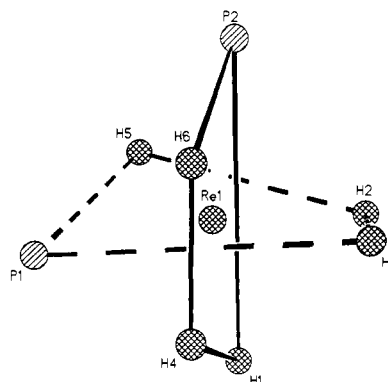**Figure 2.** Inner coordination spheres of the potassium and rhenium centers in $\{K(THF)_2ReH_6(PPh_3)_2\}_2$.

Figure 3. Idealized orthogonal trapezoidal units of the dodecahedral coordination geometry about Re in $\{K(THF)_2ReH_6(PPh_3)_2\}_2$.

used throughout the analysis;[18a] both the real ($\Delta f'$) and imaginary ($i\Delta f''$) components of anomalous dispersion[18b] were included. The quantity minimized during least-squares analysis was $\sum w(|F_o| - |F_c|)^2$ where w^{-1} = $\sigma_2(F)$ + 0.0003$(F)^2$.

The structure was solved by direct methods (SHELXTL PLUS) and refined by full-matrix least-squares techniques. Hydrogen atom contributions were included using a riding model with d(C-H) = 0.96 Å and U(iso) = 0.08 Å^2. A series of difference Fourier syntheses revealed six metal-bound hydrogen atoms. Refinement of positional and isotropic thermal parameters for these six hydrides proceeded normally to within accepted values. While hydride positions are often poorly determined by X-ray diffraction, we feel the quality of the data obtained can be relied upon for the number and angular location of the hydrides. Re-H bond lengths are however subject to systematic error. Refinement of positional and anisotropic thermal parameters (isotropic thermal parameters for

(18) *International Tables for X-ray Crystallography*; Kynoch Press: Birmingham, England, 1974; (a) pp 99-101, (b) pp 149-150.

Table I. Crystal Data for [K(THF)$_2$ReH$_6$(PPh$_3$)$_2$]$_2$

formula	C$_{88}$H$_{104}$O$_4$P$_4$K$_2$Re$_2$
fw	1800.2
cryst syst	monoclinic
space gp	$P2_1/n$
a, Å	10.987 (2)
b, Å	27.134 (4)
c, Å	14.030 (2)
β, deg	96.609 (13)
V, Å^3	4154.6 (11)
Z	2
D_{calcd}, mg/m^3	1.44
diffractometer	Syntex P2$_1$
radiation	Mo Kα ($\bar{\lambda}$ = 0.710 730 Å)
monochromator	highly oriented graphite
data colld	+h,+k,±l
scan type	coupled θ (crystal) – 2θ (counter)
scan width	symmetrical [(Kα_1) – 0.6] → [(Kα_2) + 0.6]
scan speed	2.5 deg min^{-1} (in ω)
2θ_{max}, deg	45.0
μ(Mo Kα), mm^{-1}	3.17
abspn corrn	semiempirical (ψ-scan method)
reflcns colld	5453
reflcns with $|F_o|$ > 1.0σ($|F_o|$)	4646
no. of variables	475
R_F, %	5.7
R_{wF}, %	4.6
goodness of fit	1.43
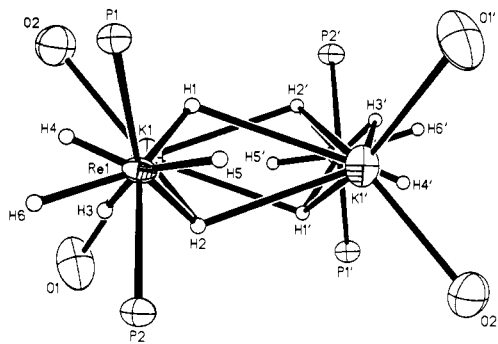
Figure 4. ORTEP view of the inner coordination spheres looking down the Re–K vectors. The staggering of the PReP and OKO planes is evident.
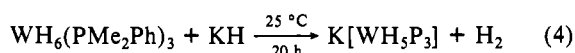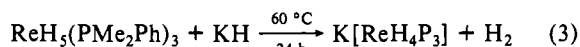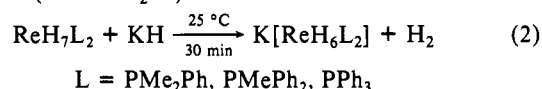
hydride atoms) led to convergence with R_f = 5.7%, R_{wF} = 4.6%, and GOF = 1.43 for 475 variables refined against those 4646 data with $|F_o|$ > 1.0σ($|F_o|$) (R_F = 4.7%, R_{wF} = 4.4% for those 4142 data with $|F_o|$ > 3.0σ($|F_o|$); R_F = 3.7%, R_{wF} = 4.0% for those 3649 data with $|F_o|$> 6.0σ($|F_o|$)). A final difference Fourier synthesis showed no significant features (ρ(max) = 0.78 e Å^{-3}). The results of the structure determination are shown in Table II, Figures 1–4, and in the supplementary material.

Results and Discussion

Synthesis of Polyhydride Anions. Transition-metal polyhydride complexes, like their boron main-group relatives,[19] can be deprotonated by the strong base KH. We reported earlier[2,7] that OsH$_4$(PMe$_2$Ph)$_3$ reacts with excess KH at 65 °C to yield H$_2$ and K[OsH$_3$(PMe$_2$Ph)$_3$] in quantitative yield (eq 1, P = PMe$_2$Ph).

$$\text{OsH}_4\text{P}_3 + \text{KH} \rightarrow \text{K[OsH}_3\text{P}_3] + \text{H}_2 \qquad (1)$$

Other polyhydride anions have now been generated by this method. The anions and the conditions employed for their synthesis are listed below (P = PMe$_2$Ph).

$$\text{ReH}_7\text{L}_2 + \text{KH} \xrightarrow[\text{30 min}]{25\ ^{\circ}\text{C}} \text{K[ReH}_6\text{L}_2] + \text{H}_2 \qquad (2)$$

$$\text{L} = \text{PMe}_2\text{Ph, PMePh}_2\text{, PPh}_3$$

$$\text{ReH}_5(\text{PMe}_2\text{Ph})_3 + \text{KH} \xrightarrow[\text{24 h}]{60\ ^{\circ}\text{C}} \text{K[ReH}_4\text{P}_3] + \text{H}_2 \qquad (3)$$

$$\text{WH}_6(\text{PMe}_2\text{Ph})_3 + \text{KH} \xrightarrow[\text{20 h}]{25\ ^{\circ}\text{C}} \text{K[WH}_5\text{P}_3] + \text{H}_2 \qquad (4)$$

(19) Shore, S. G. *Pure Appl. Chem.* **1977**, *49*, 717.

The selection of KH as the deprotonating reagent deserves some comment.[9,19] Since KH is completely insoluble in THF, toluene, and benzene, excess KH is usually employed to speed up the heterogeneous reaction. This excess KH can be simply filtered away when homogeneous solutions of the transition-metal polyhydride anion are desired. Other deprotonating agents such as MeLi, *n*-butyllithium, and 1,8-bis(dimethylamino)naphthalene (Proton Sponge) clearly do not offer this convenience. Furthermore, since all of these anions rapidly convert back to their neutral polyhydride precursors in the presence of trace amounts of H$_2$O, small amounts of KH can be added to these solutions to scavenge such protons. In effect, the KMH$_n$L$_x$/KH mixture effectively dries the solvent to precisely the degree required for reagent purity. This practice is especially useful in obtaining NMR data (where the glass surface-to-volume ratio is high) since KH shows no resonances in the NMR (due to solubility) and thus does not interfere. This could obviously not be said for *n*-butyllithium or Proton Sponge.

Characterization of Polyhydride Anions. NMR Studies of KWH$_5$(PMe$_2$Ph)$_3$ in THF. Especially informative in the characterization of the anions in eq 1–4 is the use of selective "hydride coupling" of the ^{31}P NMR spectra to determine the number of hydride ligands present. This result is achieved by decoupling only the alkyl and aryl protons of the phosphine in the ^{31}P NMR. The ^{31}P spectrum then shows coupling to the hydride ligands only and gives a $N + 1$ pattern where N equals the number of hydrides. For example, the ^{31}P{^{1}H} singlet (with W satellites) and the hydride-coupled ^{31}P NMR sextet for (THF)$_x$K[WH$_5$P$_3$] clearly demonstrate that the product from the reaction of KH with WH$_6$P$_3$ contains five hydride ligands. A limitation of this method for quantitating hydrides exists in cases where J_{MH-P} is too small to clearly resolve the number of lines. In addition, since power required for decoupling is proportional to J_{MH-P}, very small coupling constants can make *selective* decoupling unrealizable in practice.

Tetrameric aggregation is found for crystals of {LiWH$_5$-(PMe$_3$)$_3$}$_4$[5] grown from diethyl ether. Such aggregation is broken up by addition of crown ether to the potassium analogue and the complex (18-crown-6)K[WH$_5$(PMe$_3$)$_3$][5] has been found to contain a monomeric tungsten center with three hydrides bridging to potassium. Such a structure is consistent with our low-temperature NMR studies of K[WH$_5$(PMe$_2$Ph)$_3$] in THF-d_8. At 20 °C, the ^{31}P{^{1}H} NMR shows a singlet, which broadens upon cooling and finally separates to an AB$_2$ pattern at –90 °C. In the ^{1}H NMR spectrum, the hydride resonance shows fluxional behavior (Figure 5), in agreement with the formulation of three bridging and two terminal hydride ligands. At 50 °C, a bridge–terminal exchange process is rapid, giving rise to a quartet (J_{H-P} = 27 Hz). Cooling the sample to –30 °C clearly separates the hydride signal into a broad quartet integrating for three hydrides and a broad multiplet integrating for two hydrides. Further cooling (Figure 5E) collapses the broad multiplet and broadens the quartet. At –85 °C, the collapse of multiplets of –60° has resolved into two peaks, one at –4.1 ppm and the other under the –5.0 ppm resonance. The appearance of intensity 1 resonances is consistent with the 2:1:1:1 hydride pattern expected for a mirror symmetric dodecahedral (THF)$_x$K(μ-H)$_3$WH$_2$P$_3$ structure, where K$^+$ interacts with three hydrides most remote from P:
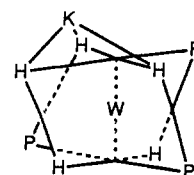
NMR Studies of (THF)$_x$KReH$_6$(PPh$_3$)$_2$ in Solution. The solid-state structure of K[OsH$_3$P$_3$][7] has recently been determined and reveals intimate ion pairs in a dimeric structure involving K–H–Os interactions. The dimerization of these anions encapsulates potassium to give a benzene-soluble species. We have explored the generality of ion pairing and dimerization with an

Transition-Metal Polyhydride Anions

J. Am. Chem. Soc., Vol. 111, No. 22, 1989   8395

Table II. Interatomic Distances (Å) and Angles (deg) with Esd's

Re1-P1	2.372 (2)	K1-H2	2.831 (66)	Re1-H6	1.647 (76)
Re1-H1	1.729 (87)	K1-H3	2.920 (71)	Re1···K1'	3.698 (2)
Re1-H3	1.149 (78)	Re1-P2	2.362 (2)	K1-H1'	2.878 (83)
Re1-H5	1.486 (74)	Re1-H2	1.632 (65)	K1-H2'	2.756 (69)
Re1···K1	3.535 (2)	Re1-H4	1.284 (78)	K1···K1'	4.151 (5)
K1-H1	2.632 (84)				
P1-C11	1.863 (8)	C44-C45	1.386 (14)	C31-C32	1.369 (13)
P1-C31	1.866 (9)	C51-C52	1.397 (13)	C32-C33	1.397 (16)
C11-C16	1.371 (12)	C52-C53	1.376 (14)	C34-C35	1.371 (18)
C13-C14	1.375 (13)	C(54)-C(55)	1.395 (15)	P2-C41	1.857 (9)
C15-C16	1.369 (14)	C(61)-C(62)	1.394 (13)	P2-C61	1.849 (9)
C21-C26	1.394 (13)	C(62)-C(63)	1.399 (14)	C41-C46	1.380 (13)
C23-C24	1.357 (15)	C64-C65	1.372 (16)	C43-C44	1.380 (14)
C25-C26	1.389 (16)	P1-C21	1.845 (9)	C45-C46	1.377 (14)
C31-C36	1.384 (14)	C11-C12	1.413 (12)	C51-C56	1.411 (12)
C33-C34	1.356 (20)	C12-C13	1.381 (13)	C53-C54	1.378 (14)
C35-C36	1.373 (15)	C14-C15	1.392 (15)	C55-C56	1.371 (14)
P2-C51	1.826 (9)	C21-C22	1.368 (12)	C61-C66	1.402 (14)
C41-C42	1.388 (12)	C22-C23	1.390 (14)	C63-C64	1.377 (18)
C42-C43	1.389 (13)	C24-C25	1.390 (16)	C65-C66	1.357 (14)
K1-O1	2.654 (9)	O2-C8	1.384 (22)	C2-C3	1.495 (21)
O1-C1	1.422 (16)	C6-C7	1.406 (28)	O2-C5	1.351 (17)
C1-C2	1.489 (21)	K1-O2	2.623 (9)	C5-C6	1.431 (24)
C3-C4	1.357 (23)	O1-C4	1.394 (19)	C7-C8	1.431 (28)
P1-Re1-P2	108.3 (1)	P2-Re1-H3	86.3 (35)	H3-Re1-H6	64.3 (44)
H1-Re1-H3	95.0 (45)	P2-Re1-H5	74.9 (29)	H5-Re1-H6	127.6 (39)
H1-Re1-H4	84.0 (44)	Re1-H1-K1	106.4 (39)	P1-Re1-H2	151.9 (24)
H3-Re1-H4	65.3 (48)	K1-H1-K1'	97.7 (24)	P1-Re1-H4	77.2 (33)
H2-Re1-H5	91.2 (35)	Re1-H2-K1'	112.3 (32)	P1-Re1-H6	87.4 (24)
H4-Re1-H5	146.1 (43)	Re1-H3-K1	113.4 (44)	P2-Re1-H2	85.1 (23)
H2-Re1-H6	120.7 (34)	H1-Re1-H2	69.0 (34)	P2-Re1-H4	123.4 (35)
H4-Re1-H6	55.1 (44)	H2-Re1-H3	61.7 (42)	P2-Re1-H6	68.7 (27)
P1-Re1-H1	89.6 (27)	H2-Re1-H4	116.7 (40)	Re1-H1-K1'	104.0 (35)
P1-Re1-H3	141.4 (35)	H1-Re1-H5	89.2 (40)	Re1-H2-K1	101.3 (28)
P1-Re1-H5	69.6 (26)	H3-Re1-H5	148.6 (43)	K1-H2-K1'	96.0 (20)
P2-Re1-H1	149.4 (27)	H1-Re1-H6	138.7 (40)		
Re1-P1-C11	115.6 (3)	C42-C43-C44	120.6 (8)	C21-C26-C25	120.2 (9)
C11-P1-C21	101.2 (4)	C44-C45-C46	121.2 (10)	P1-C31-C36	118.0 (7)
C11-P1-C31	99.5 (4)	P2-C51-C52	121.1 (6)	C31-C32-C33	120.8 (11)
P1-C11-C12	118.7 (6)	C52-C51-C56	115.6 (8)	C33-C34-C35	121.1 (11)
C12-C11-C16	117.2 (8)	C52-C53C54	121.2 (10)	C31-C36-C35	121.2 (10)
C12-C13-C14	121.9 (9)	C54-C55-C56	118.2 (9)	Re1-P2-C51	117.9 (3)
C14-C15-C16	121.7 (9)	P2-C61-C62	122.8 (7)	Re1-P2-C61	120.0 (3)
P1-C21-C22	119.3 (7)	C62-C61-C66	118.3 (8)	C51-P2-C61	101.1 (4)
C22-C21-C26	117.5 (8)	C62-C63-C64	119.9 (10)	P2-C41-C46	124.1 (6)
C22-C23-C24	119.1 (9)	C64-C65-C66	121.6 (10)	C41-C42-C43	121.2 (8)
C24-C25-C26	120.4 (10)	Re1-P1-C21	118.4 (3)	C43-C44-C45	118.0 (9)
P1-C31-C32	123.5 (8)	Re1-P1-C31	118.8 (3)	C41-C46-C45	121.2 (9)
C32-C31-C36	118.4 (9)	C21-P1-C31	99.9 (4)	P2-C51-C56	123.2 (7)
C32-C33-C34	119.2 (11)	P1-C11-C16	124.1 (7)	C51-C52-C53	121.4 (8)
C34-C35-C36	119.2 (11)	C11-C12-C13	120.3 (8)	C53-C54-C55	119.6 (9)
Re1-P2-C41	114.8 (3)	C13-C14-C15	117.1 (9)	C51-C56-C55	123.9 (9)
C41-P2-C51	99.9 (4)	C11-C16-C15	121.7 (9)	P2-C61-C66	118.9 (7)
C41-P2-C61	99.7 (4)	P1-C21-C26	123.2 (7)	C61-C62-C63	120.2 (9)
P2-C41-C42	118.3 (7)	C21-C22-C23	122.9 (9)	C63-C64-C65	119.6 (10)
C42-C41-C46	117.6 (8)	C23-C24-C25	119.8 (10)	C61-C66-C65	120.4 (9)
H1-K1-O1	143.7 (19)	H2-K1-O2	129.1 (13)	H1-K1-O2	95.3 (18)
H3-K1-O1	98.6 (16)	H2-K1-O1	107.4 (14)	H3-K1-O2	104.9 (14)
O1-K1-O2	99.3 (3)	C5-O2-C8	105.0 (11)	C1-C2-C3	104.6 (12)
K1-O1-C4	123.9 (9)	C5-C6-C7	101.1 (15)	O1-C4-C3	106.0 (12)
O1-C1-C2	101.1 (11)	O2-C8-C7	108.5 (16)	K1-O2-C8	117.8 (9)
C2-C3-C4	100.1 (13)	K1-O1-C1	120.0 (8)	O2-C5-C6	111.1 (14)
K1-O2-C5	134.7 (9)	C1-O1-C4	112.3 (11)	C6-C7-C8	106.5 (16)

examination of $K(THF)_2ReH_6(PPh_3)_2$ (**1**), which is produced according to eq 2. We first examined the solution behavior of this complex. When it is dissolved in toluene and toluene is subsequently removed in vacuo, the desolvated complex $KReH_6(PPh_3)_2$ (**2**) is isolated. This complex is also soluble in aromatic solvents. Attempts to synthesize directly the desolvated complex $KReH_6(PPh_3)_2$ by reacting KH and $ReH_7(PPh_3)_2$ in toluene solvent led to a mixture of products. The ^1H NMR spectrum of $K(THF)_2ReH_6(PPh_3)_2$ shows it to dissolve in C_6D_6 to give the unsolvated material (i.e., THF is liberated). The hydride region shows a triplet resonance (coupling to two phosphorus atoms), indicative of rapid fluxionality of the hydrogen atoms about rhenium. In an effort to slow this fluxional process, low-temperature ^1H NMR studies of $K(THF)_2ReH_6(PPh_3)_2$ and $KReH_6(PPh_3)_2$ were undertaken. When samples in toluene-d_8 were examined at 10–20-deg intervals down to −88 °C, the hydride triplets of both complexes broadened into the base line. For $K(THF)_2ReH_6(PPh_3)_2$, new resonances began to appear but were

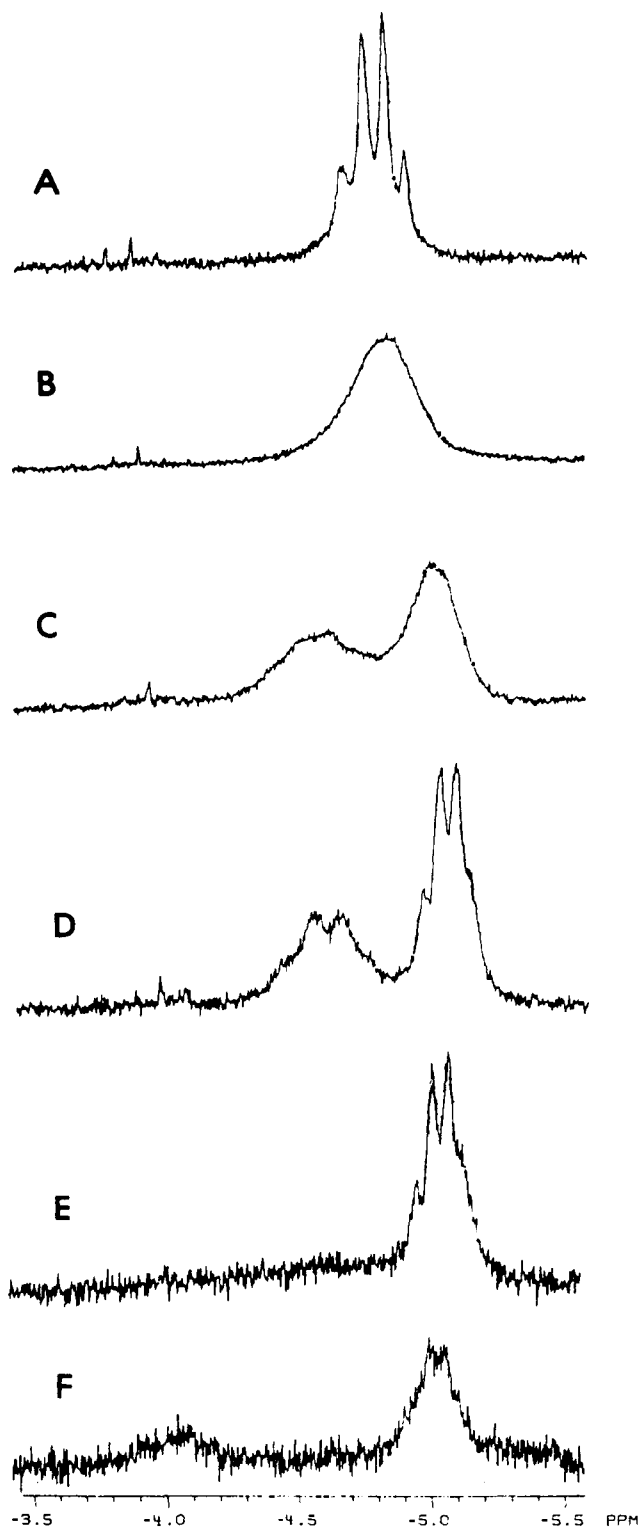**Figure 5.** Variable-temperature ^{1}H NMR spectra of $K[WH_5(PMe_2Ph)_3]$ in THF-d_8: (A) 50 °C (J_{H-P} = 27 Hz), (B) 19 °C, (C) –10 °C, (D) –30 °C, (E) –60 °C, (F) –85 °C.

not resolved before the solvent froze. Both salts are completely insoluble in hexane, which permits single-crystal growth of the solvated complex (**1**) from a 4:1 hexane/THF solution. Attempts to grow X-ray quality crystals of **2** in noncoordinating solvents were unsuccessful.

Molecular Structure of $\{K(THF)_2ReH_6(PPh_3)_2\}_2$. The X-ray study of **1** shows (Figures 1 and 2) that, in spite of coordination of two THF molecules to each potassium, dimerization occurs in the solid state. The condensation of $K(THF)_2ReH_6(PPh_3)_2$ into a centrosymmetric dimer occurs by hydride bridging. All hydrogen atoms bound to rhenium were located, establishing that three types

of hydride ligands are present. Hydrogens H1 and H2 are triply bridged to Re1, K1, and K1', lying 0.97 and 0.92 Å above and below the plane formed by the three metal atoms. Hydrogen H3 is doubly bridged to Re1 and K1 and hydrogens H4, H5, and H6 are terminally bound to Re1. None of the hydrogens are within covalent bonding distance of each other, indicating the absence of η^2-dihydrogen in the solid state. The P–Re–P angle (108.3°) is much smaller than 138.9° found in nine-coordinate ReH$_7$-(PPh$_3$)$_2$.[20] The long Re1–K1 and Re1–K1' distances of 3.535 and 3.698 Å are consistent with the absence of a direct rhenium–potassium interaction. The geometry about rhenium is eight-coordinate and may be described as a distorted dodecahedron. This geometry is most clearly defined (Figure 3) by the intersection of two perpendicular trapezoidal planes, each containing the metal center. Dodecahedral geometries have been reported for $OsH_6(P^iPr_2Ph)_2$[21] and $ReH_6(PMePh_2)_2(AlMe_2)$,[11] and the dodecahedron is reasonable in that it places the large phosphine ligands in the less hindered sites of each trapezoid. However, it must be recognized that $OsH_6(P^iPr_2Ph)_2$ has the phosphines in the *same* trapezoid, while **1** has them in two *different* trapezoids (hence the large difference in PMP angles between these two compounds, 155.2° vs 108.3°). The obvious explanation for this difference is that the structure of **1** organizes more hydrides in one hemisphere about Re, thus minimizing the steric interaction of each phosphine with the approaching *two* $K(THF)_2^+$ units. In other words, the polyhydride anion reorganizes itself in order to accommodate the increased steric encumbrance in the intimate ion pair. Similar reorganization is observed in ReH_6AlMe_2-(PMePh$_2$)$_2$ where the P–Re–P angle is 96.5°.

The aggregation in compound **1** may be attributed to the need to fill the coordination environment about potassium. In this dimeric form, potassium is seven-coordinate and is bound to three hydride ligands from one rhenium and two from the other. There are no K–C(phenyl) bonding interactions, these distances being no shorter than 3.97 Å (K'–C52). This desire for potassium to fill its coordination sphere by forming a tight ion pair has been previously reported for $KOsH_3(PMe_2Ph)_3$, where it is, however, augmented by K–phenyl bonding. Aggregation of **1** to a higher oligomer (cf. $\{LiWH_5(PMe_3)_3\}_4$) is prevented not only by bound THF but also by the bulk of PPh$_3$. The average dihedral angle of 34° between the O–K–Re and P–Re–K planes (Figure 4) shows the adoption of a staggered conformation in order to reduce steric repulsions.

Mechanism of the Polyhydride Anion Synthesis. Since the deprotonation of these neutral polyhydrides is a formal 2e reduction, complexes of a given metal in its highest oxidation state might be expected to deprotonate fastest. This observation is most clearly demonstrated by a comparison of the deprotonation conditions for ReH$_7$P$_2$ and ReH$_5$P$_3$ (eq 2 and 3). Gas evolution (H$_2$) and the formation of a yellow solution, $K[ReH_6P_2]$, are immediately observed when KH is added to a THF solution of ReH$_7$P$_2$. ReH$_5$P$_3$, on the other hand, must be heated at reflux in THF with KH for 24 h to produce $K[ReH_4P_3]$.

While our discussion of the synthetic reactions to this point has been in terms of the hydride in KH removing H$^+$ from a neutral polyhydride, a *displacement* mechanism also requires consideration. Thus, since ReH$_7$(PPh$_3$)$_2$ is known to dissociate H$_2$[22] (and ReH$_7$(PPh$_3$)$_2$ may contain H$_2$[23] and thus serve as a "good leaving group" (eq 5), perhaps via some dissociative equilibrium (eq 6)),

$$X^- + M(H_2)L_n \rightarrow MXL_n^- + H_2 \qquad (5)$$

$$M(H_2)L_n \rightleftharpoons ML_n + H_2 \qquad (6)$$
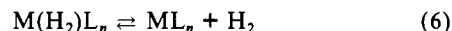
it is conceivable that certain of the polyhydride anions described here may be formed by transfer of hydride from KH to the 16e

(20) Howard, J. A. K.; Johnson, O.; Koetzle, T. F.; Spencer, J. L. *Inorg. Chem.* **1987**, *26*, 2930.

(21) Frost, R. W.; Howard, J. A. K.; Spencer, J. L. *Acta Crystallogr., Sect. C* **1984**, *40*, 946.

(22) Zeiher, E. H. K.; DeWit, D. G.; Caulton, K. G. *J. Am. Chem. Soc.* **1984**, *106*, 7006.

(23) Hamilton, D. G.; Crabtree, R. H. *J. Am. Chem. Soc.* **1988**, *110*, 4126.
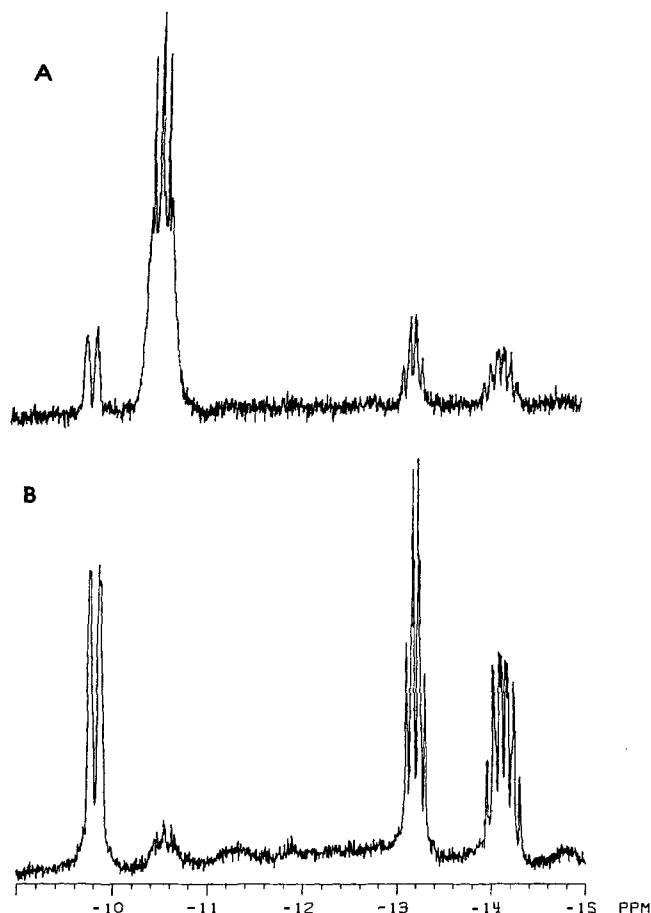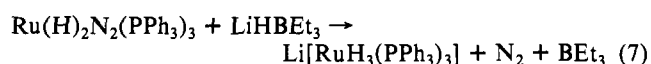
Figure 6. ^{1}H NMR (360 MHz, C_6D_6) of $(COD)RhH_3Ru(PPh_3)_3$: (A) After 30 min, $(COD)Rh(\mu-H)_3Ru(PPh_3)_3$ is the major isomer present. (B) After 2 h, $(COD)Rh(H)(\mu-H)Ru(H)(PPh_3)_3$ is the major isomer present.

participant in such an equilibrium. Such hydride transfer is made more plausible by the report[4] that H$^-$ can "displace" N$_2$ (eq 7).

$$Ru(H)_2N_2(PPh_3)_3 + LiHBEt_3 \rightarrow$$
$$Li[RuH_3(PPh_3)_3] + N_2 + BEt_3 \quad (7)$$

The distinction between these two mechanisms is made clearest by the following isotopic labeling experiment, where eq 8 is the anticipated outcome of a Brønsted acid/base mechanism and eq 9 is indicative of an η^2-H$_2$ displacement mechanism. In fact, we

$$MH_mL_n + KD \rightarrow K[MH_{m-1}L_n] + HD \quad (8)$$

$$MH_mL_n + KD \rightarrow K[MH_{m-2}DL_n] + H_2 \quad (9)$$

find that the rapid reaction of KD with ReH$_7$(PPh$_3$)$_2$ in THF, followed by prompt removal of evolved gases with a Toepler pump, gives primarily HD (mass spectrometry) and ReH$_6$(PPh$_3$)$_2^-$ containing less than 5 atom % deuterium (^{2}H NMR). Thus, displacement is not operative, and a Brønsted acid/base mechanism does occur. The recent studies by Heinekey[24] in which a ruthenium complex of coordinated H$_2$ is deprotonated (by NEt$_3$) more rapidly than is the isomeric dihydride complex would suggest that it is coordinated H$_2$ in Re(H$_2$)(H)$_5$L$_2$ that is the source of half of the diatomic H$_2$ evolved.

Heterobimetallic Polyhydride Exhibiting Slow Hydride Migration. We were particularly interested in synthesizing a heterometallic polyhydride containing two 4d metals due to the advantage of their higher kinetic reactivity compared to 5d metals. The polyhydride anion Li[RuH$_3$(PPh$_3$)$_3$] reacts with [(COD)-RhCl]$_2$ in THF to eliminate LiCl and form (COD)Rh(μ-H)$_3$Ru(PPh$_3$)$_3$ (3) in quantitative yield. Although no P–Rh

(24) Chinn, M. S.; Heinekey, D. M. *J. Am. Chem. Soc.* **1987**, *109*, 5865.
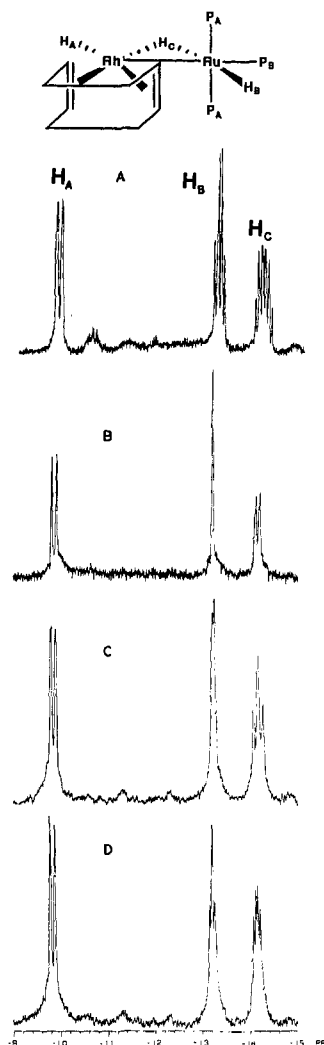
Figure 7. ^{1}H NMR (360 MHz, C_6D_6) of $(COD)Rh(H)(\mu-H)Ru(H)$-$(PPh_3)_3$: (A) completely ^{31}P coupled, (B) completely ^{31}P decoupled (^{1}H{^{31}P}; J_{H_A-Rh} = 38 Hz; J_{H_C-Rh} = 31 Hz), (C) selectively coupled to the unique phosphine (^{1}H{^{31}P$_A$}; J_{H_B-P} = 7 Hz; J_{H_C-P} = 31 H), (D) selectively coupled to the equivalent mutually trans phosphines (^{1}H{^{31}P$_B$}; J_{H_B-P} = 20 Hz; J_{H_C-P} = 17 Hz).

coupling is observed in the ^{31}P{^{1}H} NMR, 3 shows a second-order multiplet indicative of η^3 attachment of an internally rigid facial H$_3$Ru(PPh$_3$)$_3^-$ unit, as well as three resonances for the cyclooctadiene ligand. Upon standing in solution (C_6D_6) for a period of 2 h, compound 3 undergoes isomerization ($t_{1/2}$ = 40 min) to form an isomer of structure (COD)Rh(H)(μ-H)Ru(H)(PPh$_3$)$_3$ (eq 10). This isomerization can be conveniently followed by ^{1}H
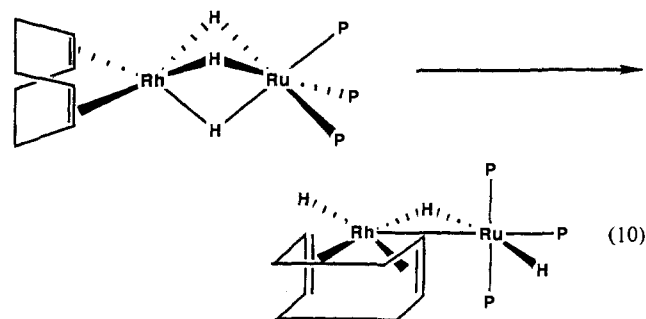
NMR spectroscopy in the hydride region (Figure 6); the resonance at −10.60 ppm for (COD)Rh(μ-H)$_3$RuPPh$_3$ slowly disappears while multiplets appear for (COD)Rh(H)(μ-H)Ru(H)(PPh$_3$)$_3$ at −14.20, −13.20, and −9.80 ppm. This structure was established by selective decoupling experiments. The *connectivity* of the RuRhH$_3$P$_3$ spin system was determined as follows: decoupling

(Figure 7) all the phosphorus ligands collapses the resonance at −14.20 ppm to a doublet ($J_{\text{H-Rh}}$ = 31 Hz), the resonance at −9.80 ppm remains unaltered as a doublet ($J_{\text{H-Rh}}$ = 38 Hz), and the signal at −13.20 ppm becomes a singlet with no rhodium coupling. The magnitude of these couplings, along with the fact that the hydride signal at −9.80 ppm shows the smallest (<2 Hz) coupling to phosphorus, indicates that this hydride is terminal on rhodium (H_A). The hydride resonance at −14.20 ppm, which shows strong coupling to both Rh and all phosphines on Ru must be bridging the Ru–Rh bond (H_C). The remaining hydride (−13.20 ppm), which lacks rhodium coupling and couples strongly to the phosphine ligands, is thus terminal on ruthenium (H_B).

Since attempts to obtain crystals suitable for X-ray diffraction were unsuccessful, the *stereochemistry* of this complex was also deduced from the NMR data. The magnitudes of the $J_{\text{H-P}}$ couplings for the hydride ligands indicate that no hydrides are trans to phosphine ligands. The ¹H NMR also reveals that a plane of symmetry is present that produces only six chemical shifts for the 12 cyclooctadiene protons. Assuming the presence of a Rh–Ru bond and an octahedral d^6 Ru center, which is consistent with the complex being rigid on the NMR time scale, the structure in eq 10 is proposed.

This structure is further supported by the ³¹P NMR, which reveals that only the phosphine trans to the proposed Ru–Rh bond shows Rh coupling ($J_{\text{P-Rh}}$ = 10 Hz). The mutually trans phosphines show no coupling to rhodium. The formation of this thermodynamic product represents a novel case where hydride transfer (intramolecular migration) is a kinetically slow process. Moreover, no rapid hydride migration occurs in the thermodynamic product **3**.

Conclusions

Deprotonation of neutral transition-metal polyhydrides with KH in THF serves as a high yield and convenient route to po-

tassium salts of polyhydride anions. The accumulated evidence is that such "salts" are actually intimate ion pairs, with hydride ligands being sufficiently basic to compete effectively with THF for coordination sites on K⁺. Conventional coordination geometries (octahedral, dodecahedral, etc.) are retained at the transition metal even in the presence of such hydride bridging. Although the above polyhydride anions can result from abstraction of terminal hydride ligands as H⁺, there is evidence[24] that coordinated H_2 (as in $Re(H_2)(H)_5L_2$) may be deprotonated more rapidly. Polyhydride anions are sufficiently nucleophilic to react cleanly with transition-metal halogen bonds at temperatures low enough to allow detection of kinetic products before they rearrange to the thermodynamic product. Given the common occurrence of rapid hydride migration in mononuclear and polynuclear transition-metal complexes, the rearrangement of $(COD)Rh(\mu\text{-}H)_3Ru(PPh_3)_3$ to $(COD)Rh(H)(\mu\text{-}H)RuH(PPh_3)_3$ is unexpectedly slow. Moreover, since the kinetic product has three Ru–H bonds while the thermodynamic product has only two, the reaction clearly does not occur by a least motion mechanism.

Supplementary Material Available: Tables of atomic positional parameters and anisotropic thermal parameters (4 pages); listing of observed and calculated structure factors for {K-(THF)₂ReH₆(PPh₃)₂}₂ (18 pages). Ordering information is given on any current masthead page.

The Copper-Catalyzed Redox Reaction between Aqueous Hydrogen Peroxide and Hydrazine. 1. New Experimental Results and Observations

Yaping Zhong and Phooi K. Lim*

Contribution from the Department of Chemical Engineering, North Carolina State University, Raleigh, North Carolina 27695-7905. Received April 3, 1989

Abstract: Important new data are reported which make it possible to deduce the most probable mechanism of the copper-catalyzed redox reaction between aqueous hydrogen peroxide and hydrazine: $2H_2O_2 + N_2H_4 \rightarrow 4H_2O + N_2$. The reaction is marked by an induction period τ_e which varies inversely with the catalyst concentration but essentially independently with the peroxide and hydrazine concentrations. Trace amounts of cerium ion, hydroquinone, quinone, and o-phenylenediamine promote the reaction markedly. Ultrasonication accelerates the reaction, whereas a viscosity increase in the reaction solution has the opposite effect. Maleate ion produces a quantitative increase in nitrogen output above the stoichiometric equivalent of peroxide. The reaction shows no wall effect. The nitrogen and peroxide profiles and the rate are described, respectively, by

$$\frac{N_{N_2}}{V} = \frac{1}{2}([H_2O_2]_0 - [H_2O_2]) = \frac{[H_2O_2]_0}{2}\left[1 - \left(\frac{b+1}{b+e^{t/\tau_e}}\right)^c\right]$$

$$\frac{1}{V}\frac{dN_{N_2}}{dt} = \frac{k_e[Cu]_T[H_2O_2]e^{t/\tau_e}}{b + e^{t/\tau_e}}$$

$$\tau_e = m\frac{1}{[Cu]_T}$$

where b, c, k_e, and m are parameters whose empirical values at 25 °C are reported. The fundamental significance of the parameters and their interrelationships are given in the following paper.

I. Introduction

Hydrazine and its substituted cousins have attracted a long and sustaining interest among chemists and chemical engineers on

account of their importance as a fuel and chemical reagents.[1-9] Several books and review articles[1-9] and numerous papers[10-21] have

* To whom correspondence should be addressed.